Physical Layer Security of a Dual-Hop Regenerative Mixed RF/UOW System

Elmehdi Illi, Faissal El Bouanani, *Member, IEEE,* Daniel Benevides da Costa, *Senior Member, IEEE,* Paschalis C. Sofotasios, *Senior Member, IEEE,* Fouad Ayoub, *Member, IEEE,* Sami Muhaidat, *Senior Member, IEEE*, and Kahtan Mezher, *Senior Member, IEEE*

Abstract—Ensuring physical layer security is a crucial task in conventional and emerging communication systems, which are typically characterized by stringent quality of service and security requirements. This also accounts for wireless technologies in the context of the Internet of Things paradigm, which are expected to exhibit considerably increased computational complexity. Based on this, the present contribution investigates the secrecy outage performance of a dual-hop decode-and-forward (DF) mixed radio-frequency/underwater optical wireless communication (RF/UOWC) system. Such wireless network configurations are particularly useful in efficient and demanding scenarios, such as military communications. Therefore, our analysis considers one single-antenna source node (S) communicating with one legitimate destination node (D) via a DF relay node (R) equipped with multiple antennas for reception. Particularly, the relay receives the incoming signal from S via an RF link, applies selection-combining (SC) technique, fully decodes it, encodes it again and then forwards it to the destination via a UOWC link. The communication is performed under the eavesdropper's attempt to intercept the $S-R$ hop (RF side). In this context, a closed-form expression for the secrecy outage probability is derived along with a thorough asymptotic analysis in high SNR regime, based on which the achievable diversity order is provided. The offered results provide useful insights on the impact of some key system and channel parameters on the secrecy outage performance, such as the number of eavesdroppers, the number of relay antennas, fading severity parameters of RF links, and water turbulence severity of the UOWC link. The conducted analysis shows that the secrecy outage probability is dominated only by the R-D link in high SNR regime, regardless of the S-R parameters, such as the number of relay antennas and the average SNR at the relay branches. The offered analytic results are corroborated with respective results from computer simulations. Since these parameters are closely related with the computational complexity at the involved terminals, the offered insights are useful for the design and deployment of such systems.

Index Terms—Dual-hop relaying, performance analysis, physical layer security, secrecy outage probability, selection combining, underwater optical wireless communication (UOWC).

1 Introduction

With the tremendous evolution of wireless communication systems in the recent era, security and privacy concerns in wireless networks have attracted a considerable attention from the research community, as the wireless communication industry keeps prospering worldwide. Such interests are increasing due to the broadcast nature of the wireless RF link, rendering it vulnerable to intrusion threats of potential eavesdropping devices, which aim at overhearing the legitimate communication channel [1]. The traditional security practice in most current communication networks is viewed as implementing authentication and encryption protocols at higher layers. By doing so, these security designs are performed assuming ideal security at the physical layer (PHY) and error-free wireless transmission. Based on this, quantifying the physical layer security in emerging wireless communication systems has been a research theme of paramount importance in information security and wireless communication [2]. Interestingly, while higher layers consider the security aspect as an implementation of cryptographic protocols, the physical layer security paradigm, introduced pioneeringly by Wyner in [3], aims at establishing perfectly secure communication, by exploiting the random characteristics of the wireless channel, alongside with channel coding as well as spatial diversity [2], [4], [5], [6]. Nevertheless, this process increases the required computation complexity, which is critical in large-scale systems and autonomous devices and terminals. As a result, precise determination of physical layer security is essential in order to subsequently allow the quantification of the overall computational requirements of future wireless technologies and ensure that these are maintained within realistic and sustainable levels.

With the dramatic increase of human activities in the underwater environments [7] in the last two decades, un-

- *E. Illi and F. El Bouanani are with ENSIAS College of engineering, Mohammed V University in Rabat, Morocco (e-mails: {elmehdi.illi, f.elbouanani}@um5s.net.ma).*
- *D. B. da Costa is with the Department of Computer Engineering, Federal University of Ceará (UFC), Sobral-CE, Brazil (e-mail: danielbcosta@ieee.org).*
- *P. C. Sofotasios is with the Department of Electronics and Communications Engineering, Tampere University of Technology, FI-33720, Tampere, Finland (e-mail: paschalis.sofotasios@tut.fi).*
- *F. Ayoub is with CRMEF, Kenitra, Morocco (e-mail: ayoub@crmefk.ma).*
- *S. Muhaidat is with the Institute for Communication Systems, University of Surrey, Guildford GU2 7XH, United Kingdom (e-mail: muhaidat@ieee.org).*
- *K. Mezher, Department of Electrical and Computer Engineering, Khalifa University of Science and Technology, 127788, Abu Dhabi, UAE (e-mail: kahtan.mezher@ku.ac.ae).*

derwater wireless communication technology has gained a great interest as it enables the realization of several potential applications, e.g., oil production and control, ecological monitoring, climate recording, and military surveillance [8]. Yet, neither the traditional acoustic nor radio-frequency (RF) technologies seem capable of providing high-speed underwater communications [9], because of their limited bandwidth. Moreover, the acoustic link suffers from communication delays; as a result, deploying real-time high-speed underwater applications via acoustic technology remains a challenging objective to achieve [7]. From another front, underwater optical wireless communication (UOWC) technology has also received considerable attention, as a promising key-enabling technology for large volume high-speed underwater communications [10]. While acoustic communication provides a very low data rate and serious communication delays, UOWC technology may offer a data rate up to tens of Gbps at moderate propagation distance (tens of meters) [9]. Additionally, high communication security, low latency, and energy efficiency endorse optical communication as a widely accepted and appropriate communication solution in the underwater medium [8]- [10] and the references therein.

It is recalled that relaying technology has been widely advocated as a practical solution for long-range communications, as it provides wider network coverage as well as increased communication system's capacity [11]. As such, significant research attention has been devoted to the analysis of dual-hop and multi-hop relaying communication systems. The main principle in these cooperative wireless network architectures is to place one or multiple relay node(s), in order to forward the transmitted information signal from the source to the destination, over two or several time slots. The transmission protocol can be performed with either regenerative or non-regenerative relaying scheme. The latter, known also as amplify-and-forward (AF), is less complex as it is based on amplifying the signal at the relay with either a fixed gain or a variable gain prior to forwarding it to the destination, while regenerative decode-and-forward (DF) scheme lies on fully decoding and processing the received signal, before handing it on to the destination node [12]. In contrast to AF which amplifies the received signal, in the analog domain, DF based-relaying aims at mitigating the noise effect by decoding the received binary signal, re-encoding it, and then forwarding it to the end receiver [13]. Additionally, AF does not achieve good performance in low SNR regimes due to noise amplification. Interestingly, selective DF (SDF) protocol is more robust compared to the AF one. Particularly, the relay node in SDF relaying protocol forwards the received sequence or keep silence based on a certain criterion, such as error detection codes based criterion [14]. Furthermore, conventional DF relay-based protocol is more energy efficient than its AF counterpart [15]. However, practically, hardware suffers from several types of impairments, such as phase noise, I/Q imbalance, as well as high power amplifier nonlinearities among others [16].

Due to the limitations of terrestrial free-space-optical (FSO) links caused by atmospheric turbulence, mixed dual-hop RF/FSO systems have been widely investigated in the literature as an effective solution to mitigate optical channel's limitations. In this mixed configuration, the source node communicates through an RF link with the relay, which by its turn, converts the received signal into an optical light wave and delivers it through an FSO link to the destination. In this context, the authors in [17] conducted a performance analysis of a dual-hop mixed RF/FSO system, where the respective links were subject to Nakagami-m and Gamma-Gamma fading conditions. Likewise, similar analyses were conducted in [18], [19], taking into consideration the realistic Málaga-$\mathcal{M}$ and Double Generalized-Gamma FSO turbulence fading conditions, respectively.

As aforementioned, there has been an increasing interest currently in the security investigation of communication systems over fading channels. This topic is critical because different fading conditions between the involved terminals in a wireless network result to variations of the achieved security levels.

Therefore, it is essential to provide accurate quantification of the achievable physical layer security in order to design and deploy such systems efficiently. Importantly, this also concerns the corresponding computational complexity associated with the estimation of the fading parameters and the determination of the security levels. This complexity has to be within tolerable and sustainable limits, which is a key challenge in modern and versatile wireless systems and networks. For that purpose, the authors in [20] analyzed the secrecy performance of a multiple-input multiple-output (MIMO) system, subject to Nakagami-m fading, with the presence of a multiple-antenna eavesdropper, while in [21], [22], the secrecy performance in a multi-user and multi-eavesdropper cellular network was investigated. In addition, the work in [23] dealt with the secrecy analysis of a land mobile satellite communication system. Besides, several contributions, such as in [24], [25], and [26], dealt with the secrecy performance of FSO links. In contrast to the RF link that is vulnerable to eavesdropping attack due to its broadcast nature, wireless optical links (FSO/UOW) provide higher security due to their highly directional light beam. As such, analyzing the physical layer security of the mixed RF/FSO and RF/UOWC systems is necessary, since the RF hop can be easily attacked. Based on this, the authors in [27] analyzed the secrecy performance in terms of average secrecy rate and secrecy outage probability of the mixed system proposed in [17], while [28], addressed the secrecy analysis for a multi-user multi-eavesdropper RF/FSO system. Moreover, in [29], a secrecy analysis of a mixed RF/UOWC system was performed, where closed-form expressions for the intercept probability and average secrecy capacity were derived, for both fixed and variable gain relay schemes.

Motivation and contributions

The secrecy performance of mixed RF-optical links is still in its infancy, as there are only a few contributions that have addressed the secrecy analysis of these systems. In the open literature, the vast majority of the works analyzed exclusively mixed RF/FSO systems. Owing to this fact, herein we aim to determine the secrecy outage probability performance of an RF/UOWC system configuration with a multiple-antenna DF relay and in the presence of multiple

eavesdroppers. In the considered setup, the source node which consists of a distant terrestrial control station, a ship on sea, or a satellite communicates with an underwater destination node (e.g., submarine, sensor) through a moving relay node. The relay forwards to the destination node through a UOW link the broadcasted signal from the source, after decoding and re-encoding it. The adopted configuration is of practical use in relay-based wireless sensors networks in commercial as well as military applications [30], [31]. In the considered analysis, we have opted for using SC receiver. Indeed, SC combiner selects among its receive branches the one with strongest received power, while MRC receiver aims at optimally combining the received signals by employing channel state information (CSI). Even though MRC technique outperforms the SC one in terms of performance, its post detection combining requires all of RF chains at the receiver to be active always [32]. For these reasons, SC post processing remains less complex, as only a single RF chain is used. Furthermore, previous related works in [29], [33] dealt only with MRC receiver. Owing to this fact, this work aims to fill partly the gap that exists in the literature by investigating the secrecy performance of the considered system using SC technique alongside with DF relaying.

Since UOWC often requires a direct line of sight (LOS) link, the relay node moves along the sea surface in order to track continuously the destination node, thus ensuring a LOS link. In this conducted analysis, channel turbulence parameters, the number of antennas, detection technique type as well as the number of eavesdroppers are taken into account.

The main contributions of this paper are summarized below:

- Derivation of the statistics of the end-to-end signal-to-noise ratio (SNR) of the legitimate link as well as the overall wiretap channel SNR.
- The secrecy outage probability performance of the considered network is evaluated as a function of the system and channel's parameters. Specifically, in contrast to [29] and [33] where average secrecy capacity and intercept probability were derived for AF relaying scheme with consideration of MRC scheme at the relay, herein an exact closed-form expression for secrecy outage probability (SOP) of the DF protocol and assuming selection combining (SC) scheme is provided, in terms of the hypergeometric incomplete Fox's H-function.
- Relying on the residues theorem, an alternative exact closed-form expression for the SOP is provided, by expressing the Fox's H-function as a sum of elementary functions.
- An asymptotic analysis of the derived SOP expression is carried out at high SNR regime, based on which the achievable diversity order is provided.
- The derived analytical results quantify the effect of key system parameters on the secrecy performance, such as the number of relay antennas, RF fading severity parameter of the legitimate and the wiretap links, eavesdroppers received power, as well as water turbulence severity parameters of the UOWC link.

The offered results are expected to provide useful insights on the design and deployment of future systems. The remainder of this paper is organized as follows. Section 2 introduces the system and channel models, while in Section 3, statistical properties for the considered communication network are derived. In Section 4, analytical expression for the SOP alongside with its asymptotic expansion are derived, whereas Section 5 shows some illustrative numerical examples, followed by insightful discussions. Finally Section 6 concludes the paper with perspectives for future work.

2 System and Channel Models

A dual-hop mixed communication system operating under mixed RF and UOWC technologies is considered. As shown in Fig. 1, the information signal is transmitted from the source node S (e.g., ground control station, boat), via an RF link, through a DF relay node R (e.g., floating buoy), that combines the received signal copies at its N_r receive antennas using selection combining (SC) technique. After fully decoding the combined signal, the relay forwards it to the legitimate underwater destination node D (e.g., submarine) via a UOWC link. The transmission is performed in the presence of multiple eavesdroppers attackers attempting to overhear the RF side of the communication link. Since the S-R link (e.g., ground station to floating buoy) is an RF link, the source broadcast the information signal so as to reach the distant relay node. Interestingly, Nakagami-m fading is a more convenient distribution for modeling the fading amplitude in a land-mobile channel as well as scintillating ionospheric radio links. Moreover, it includes some well-known fading distributions, namely Rayleigh and Rician as special cases, and AWGN as a limit case [34].

2.1 Source-Relay hop

The $S-R$ link's signal envelope is modeled by a Nakagami-m flat fading model. As a result, the SNR γ_i received at ith antenna A_i of R is Gamma distributed with probability density function (PDF) given by [34]

$$f_{\gamma_i}(z) = \sigma_i^{m_i} \frac{z^{m_i-1}}{\Gamma(m_i)} \exp(-\sigma_i z), z > 0, i = 1, .., N_r, \quad (1)$$

where $\Gamma(.)$ denotes the Gamma function [35, Eq. (8.310.1)], $\sigma_i = \frac{m_i}{\overline{\gamma}_i}$, and $m_i \geq \frac{1}{2}$ and $\overline{\gamma}_i > 0$ denote the Nakagami-m fading parameter and the average SNR of the $S - A_i$ link, respectively. The case of independent and identically distributed (i.i.d) diversity branches, that is $m_i = m$ and $\overline{\gamma}_i = \overline{\gamma}$, is considered.

Based on this, the relay node combines the received signal from S by using its N_r antennas and the selection combining (SC) diversity technique. The total SNR γ_{SR} at the output of the SC combiner is expressed as

$$\gamma_{SR} = \max_{1 \leq i \leq N_r} \gamma_i. \quad (2)$$

Furthermore, the PDF of the SNR γ_{SR}, are given by [36]

$$f_{\gamma_{SR}}(z) = \frac{N_r \sigma^m}{(\Gamma(m))^{N_r}} \gamma_{inc}^{N_r-1}(m, \sigma z) z^{m-1} \exp(-\sigma z), \quad (3)$$

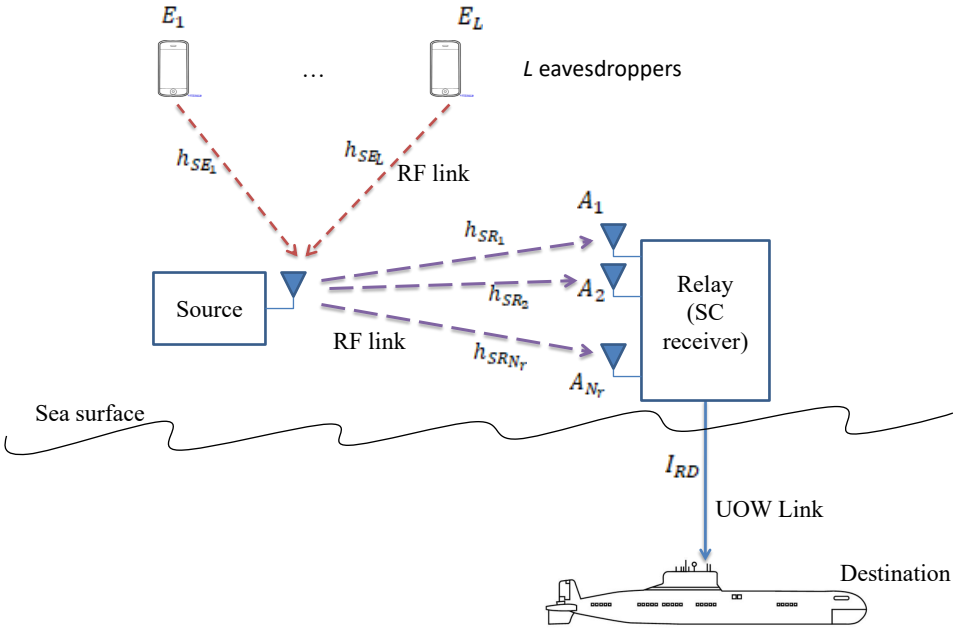

Fig. 1: System model.

where $\gamma_{inc}(.,.)$ denotes the lower incomplete Gamma function [35, Eq. (8.350.1)], and $\sigma = \frac{m}{\overline{\gamma}}$.

Consequently, the CDF of γ_{SR} can be derived readily by integrating the PDF (3) as follows

$$F_{\gamma_{SR}}(z) = \left(\frac{\gamma_{inc}(m, \sigma z)}{\Gamma(m)}\right)^{N_r}, \tag{4}$$

2.2 Source-Eavesdropper hop

The wiretap link consists of $L \geq 1$ eavesdroppers $(E_i)_{1 \leq i \leq L}$. Similarly, the links $S - E_i$ are supposed to undergo i.i.d Nakagami-m fading with PDF given by

$$f_{\gamma_{SE_i}}(z) = \sigma_e^{m_e} \frac{z^{m_e - 1}}{\Gamma(m_e)} \exp(-\sigma_e z), z > 0, \tag{5}$$

where $\sigma_e = \frac{m_e}{\overline{\gamma}_e}$, and $m_e \geq \frac{1}{2}$ and $\overline{\gamma}_e > 0$ denote the Nakagami-m fading parameter and the average SNR of the wiretap link between S and the eavesdropper node E_i, respectively.

Similarly to (4), the CDF of the S-E_i link between the source node and an eavesdropper E_i among the L eavesdroppers is given by

$$F_{\gamma_{SE_i}}(t) = \frac{\gamma_{inc}(m_e, \sigma_e t)}{\Gamma(m_e)}. \tag{6}$$

2.3 Relay-Destination hop

As already mentioned, the $R - D$ hop is a UOWC link, modeled by the mixture Exponential-Gamma model, where the PDF of the received light irradiance I_{RD} is given by [8]

$$f_{I_{RD}}(I) = \frac{\omega}{\lambda} \exp\left(-\frac{I}{\lambda}\right) + (1 - \omega) I^{\alpha - 1} \frac{\exp\left(-\frac{I}{\beta}\right)}{\beta^{\alpha} \Gamma(\alpha)}, I > 0, \tag{7}$$

with ω denoting the mixture weight factor, such that $\omega \in [0, 1]$, $\alpha > 0$ and $\beta > 0$ represent Gamma distribution's shape and scale parameters, respectively, and $\lambda > 0$ accounts for the Exponential distribution's mean.

The relationship between the irradiance and the SNR can be expressed as [11]

$$\gamma_{RD} = \frac{(\eta I_{RD})^r}{N_0}, \tag{8}$$

where $0 < \eta < 1$ refers to the photodetector efficiency, r is a detection technique-dependent parameter (e.g., $r = 1$ refers to coherent detection, while $r = 2$ stands for intensity modulation/direct detection (IM/DD) technique), and $N_0 > 0$ denotes additive white Gaussian noise's (AWGN) power spectral density.

By applying the Jacobi transform on the PDF of I_{RD} expressed in (7), and after some algebraic manipulations, we obtain the PDF of the SNR γ_{RD}, namely

$$f_{\gamma_{RD}}(z) = \omega U(1, \lambda) + (1 - \omega) U(\alpha, \beta), z > 0, \tag{9}$$

with

$$U(x, y) = \frac{1}{r \Gamma(x)} \left(\frac{\kappa_r}{y}\right)^x z^{\frac{x}{r} - 1} \exp\left(-\frac{\kappa_r}{y} z^{\frac{1}{r}}\right), \tag{10}$$

where $\kappa_r = \frac{\mathbb{E}[I]}{\mu_r^{\frac{1}{r}}}$, with $\mathbb{E}[I]$ denoting the average value of the received light irradiance defined as

$$\mathbb{E}[I] = \omega\lambda + (1 - \omega)\alpha\beta, \tag{11}$$

and $\mu_r > 0$ stands for the average electrical SNR, which is given by

$$\mu_r = \frac{\eta^r}{N_0} \mathbb{E}^r[I]. \tag{12}$$

3 USEFUL STATISTICAL PROPERTIES

A closed-form expression for the CDF of the total end-to-end SNR of the considered mixed RF/UOWC system is presented in this section.

Since the relay node performs a decode-and-forward relaying, the total received SNR at D is expressed as [12]

$$\gamma_{eq} = \min\left(\gamma_{SR}, \gamma_{RD}\right). \tag{13}$$

Given the above expression, the CDF of the SNR γ_{eq} can be expressed as follows

$$\begin{aligned} F_{\gamma_{eq}}(t) &= \Pr\left[\min\left(\gamma_{SR}, \gamma_{RD}\right) < t\right], \\ &= 1 - \left(1 - F_{\gamma_{SR}}(t)\right)\left(1 - F_{\gamma_{RD}}(t)\right), \\ &= F_{\gamma_{SR}}(t) + F_{\gamma_{RD}}(t) - F_{\gamma_{SR}}(t) F_{\gamma_{RD}}(t), \end{aligned} \tag{14}$$

where $F_{\gamma_{SR}}(t)$ is given in (4), and $F_{\gamma_{RD}}(t)$ can be readily determined as follows:

$$\begin{aligned} F_{\gamma_{RD}}(t) &= \int_0^t f_{\gamma_{RD}}(z)\, dz, \\ &= \omega\left(1 - \exp\left(-\frac{\kappa_r}{\lambda} t^{\frac{1}{r}}\right)\right) + (1-\omega)\frac{\gamma_{inc}\left(\alpha, \frac{\kappa_r}{\beta} t^{\frac{1}{r}}\right)}{\Gamma(\alpha)}. \end{aligned} \tag{15}$$

It is noted that (14) depicts an exact analytical expression for the CDF of the total end-to-end SNR assuming a DF relaying scheme. This allows us to evaluate the system outage probability, without considering the wiretap link, in terms of key system parameters, such as an arbitrary number of relay antennas, integer fading parameter of the RF hop (i.e., $(m, m_e) \in \mathbb{N}^2$), water turbulence severity parameters, and average SNR per-hop.

4 SECRECY ANALYSIS

The exact SOP of the considered RF/UOWC system is derived in this section along with its asymptotic expansion at the high SNR regime.

4.1 Secrecy outage probability

This security metric is defined as the probability that the secrecy capacity, which is the difference between the capacity of the main link (i.e., $S-R-D$ link) and that of the wiretap link, falls below a certain threshold rate R. In this case, the eavesdropper most likely achieves interception of the confidential message. SOP corresponds mathematically to an event where the difference between the main and wiretap link secrecies is in outage, being namely expressed as

$$P_{sop} = \Pr\left(C_R - C_E < R\right), \tag{16}$$

where

$$C_R = \log_2\left(1 + \gamma_{eq}\right), \tag{17}$$

and C_E denote, the channel capacities of the $S-R-D$ and $S-E$ links, respectively.

To this effect, we consider a scenario composed by L independent and non-coordinating eavesdroppers. The eavesdroppers aim to intercept independently the transmitted signal from S via an RF link. Consequently, the overall capacity of the wiretap channel from S to E is the maximum of the achievable individual capacities by the L eavesdroppers, i.e.,

$$C_E = \max_{i=1,..,L}\left(C_{SE_i}\right), \tag{18}$$

where C_{SE_i} denotes the $S-E_i$ link capacity.

Since the maximum of the individual capacities $(C_{SE_i})_{1\le i\le L}$ corresponds to the maximum SNR of the links $S-E_i$, it follows that

$$\gamma_{SE} = \max_{i=1,..,L}\left(\gamma_{SE_i}\right). \tag{19}$$

From above, the CDF of the overall wiretap link's SNR γ_{SE} can be expressed as

$$\begin{aligned} F_{\gamma_{SE}}(z) &= \Pr\left[\max_{i=1,..,L}\left(\gamma_{SE_i}\right) < z\right] \\ &= \left(\frac{\gamma_{inc}\left(m_e, \sigma_e z\right)}{\Gamma\left(m_e\right)}\right)^L. \end{aligned} \tag{20}$$

By plugging (17) and (18) into (16), and by making some algebraic manipulations, we obtain

$$\begin{aligned} P_{sop} &= \Pr\left(\gamma_{eq} < \left(2^R(\gamma_{SE}+1) - 1\right) \middle| \gamma_{SE}\right) \\ &= \int_0^\infty F_{\gamma_{eq}}\left(2^R(z+1) - 1\right) f_{\gamma_{SE}}(z) dz, \end{aligned} \tag{21}$$

with $f_{\gamma_{SE}}(z)$ denoting the PDF of the overall wiretap link, obtained by differentiating (20) with respect to z as

$$f_{\gamma_{SE}}(z) = \frac{L\sigma_e^{m_e}}{\Gamma^L\left(m_e\right)}\left[\gamma_{inc}\left(m_e, \sigma_e z\right)\right]^{L-1} e^{-\sigma_e z} z^{m_e - 1}. \tag{22}$$

Proposition 1. *For integer values of m and m_e, the SOP of the considered communication system employing DF relaying scheme is given as*

$$\begin{aligned} P_{sop} = {} & \frac{L\sigma_e^{m_e}}{\Gamma\left(m_e\right)} \sum_{u_1=0}^{L-1} \binom{L-1}{u_1} e^{-\rho}(-1)^{u_1} \sum_{u_2=0}^{u_1} .. \sum_{u_{m_e}=0}^{u_{m_e-1}} \\ & \times \prod_{h=0}^{m_e-1} \binom{u_{h+1}}{u_{h+2}} \left(\frac{1}{h!}\right)^{u_{i+1}-u_{i+2}} \sigma_e^{\delta_u} \\ & \times \sum_{i=0}^{\delta_u+m_e-1} \binom{\delta_u + m_e - 1}{i} \frac{\left(1-2^R\right)^{\delta_u+m_e-1-i}}{2^{R(\delta_u+m_e)}} \\ & \times \left(\omega\left(T_2^{(i)} + T_4^{(i)}\right) + (1-\omega)\left(T_1^{(i)} + \frac{T_3^{(i)} - T_5^{(i)}}{\Gamma(\alpha)}\right)\right) \end{aligned} \tag{23}$$

with

$$\begin{aligned} T_1^{(i)} = {} & \sum_{v_1=0}^{N_r} \binom{N_r}{v_1} (-1)^{v_1} \sum_{v_2=0}^{v_1} .. \sum_{v_m=0}^{v_{m-1}} \prod_{p=0}^{m-1} \binom{v_{p+1}}{v_{p+2}} \\ & \times \left(\frac{1}{p!}\right)^{v_{p+1}-v_{p+2}} \sigma^{\theta_v} \frac{\Gamma\left(i + \theta_v + 1, \left(2^R - 1\right)\varepsilon\right)}{\varepsilon^{\theta_v + i + 1}}, \end{aligned} \tag{24}$$

$$T_2^{(i)} = \frac{\Gamma\left(i+1, \varphi\left(2^R - 1\right)\right) - \Psi_1\left(\varphi, 0\right)}{\varphi^{i+1}}, \tag{25}$$

$$T_3^{(i)} = \frac{\Psi_2(\varphi, 0)}{\varphi^{i+1}}, \tag{26}$$

$$T_4^{(i)} = \sum_{v_1=0}^{N_r} \binom{N_r}{v_1} (-1)^{v_1} \sum_{v_2=0}^{v_1} \cdot\cdot \sum_{v_m=0}^{v_{m-1}} \prod_{p=0}^{m-1} \binom{v_{p+1}}{v_{p+2}} \times \left(\frac{1}{p!}\right)^{v_{p+1}-v_{p+2}} \sigma^{\theta_v} \frac{\Psi_1(\varepsilon, \theta_v)}{\varepsilon^{\theta_v+i+1}}, \tag{27}$$

$$T_5^{(i)} = \sum_{v_1=0}^{N_r} \binom{N_r}{v_1} (-1)^{v_1} \sum_{v_2=0}^{v_1} \cdot\cdot \sum_{v_m=0}^{v_{m-1}} \prod_{p=0}^{m-1} \binom{v_{p+1}}{v_{p+2}} \times \left(\frac{1}{p!}\right)^{v_{p+1}-v_{p+2}} \sigma^{\theta_v} \frac{\Psi_2(\varepsilon, \theta_v)}{\varepsilon^{\theta_v+i+1}}, \tag{28}$$

$$\Psi_1(\tau, \zeta) = M_{1,1}^{1,1}\left(g(\tau, \lambda) \middle| \begin{matrix} \Lambda; - \\ (0,1,0); - \end{matrix}\right), \tag{29}$$

$$\Psi_2(\tau, \zeta) = M_{2,2}^{1,2}\left(g(\tau, \beta) \middle| \begin{matrix} \Lambda, (1,1,0); - \\ (\alpha,1,0); (0,1,0); - \end{matrix}\right), \tag{30}$$

$$\Lambda = (-\zeta - i, 1/r, \tau(2^R - 1)), \tag{31}$$

$$\rho = \sigma_e(u_1 + 1)\left(\frac{1}{2^R} - 1\right), \tag{32}$$

$$\varphi = \frac{\sigma_e(u_1 + 1)}{2^R}, \tag{33}$$

$$\varepsilon = \varphi + v_1\sigma, \tag{34}$$

with

$$\theta_v = \sum_{k=1}^{m-1} k(v_{k+1} - v_{k+2}), \tag{35}$$

$$\delta_u = \sum_{k=1}^{m_e-1} k(u_{k+1} - u_{k+2}), \tag{36}$$

$$g(z, t) = \frac{\kappa_r}{t}\, z^{-\frac{1}{r}}, \tag{37}$$

where z and t can take two possible values as $z = \{\varepsilon, \varphi\}$ and $t = \{\lambda, \beta\}$, and $M_{p,q}^{m,n}\left(\Omega \middle| \begin{matrix} \Theta_1 \\ \Theta_2 \end{matrix}\right)$ is the upper incomplete Fox's H-function defined as [37]

$$M_{p,q}^{m,n}\left(\Omega \middle| \begin{matrix} \Theta_1 \\ \Theta_2 \end{matrix}\right) = \frac{1}{2\pi j}\int_{\mathcal{C}} \frac{\prod_{k=1}^{m}\Gamma(b_k + B_k s, \beta_k)}{\prod_{k=m+1}^{q}\Gamma(1 - b_k - B_k s, \beta_k)} \times \frac{\prod_{i=1}^{n}\Gamma(1 - a_i - A_i s, \alpha_i)}{\prod_{i=n+1}^{p}\Gamma(a_i + A_i s, \alpha_i)}\Omega^{-s} ds, \tag{38}$$

with $\Theta_1 = (a_i, A_i, \alpha_i)_{i=1:p}$, $\Theta_2 = (b_k, B_k, \beta_k)_{k=1:q}$, $j = \sqrt{-1}$, and $\mathcal{C}$ is a complex contour of integration ensuring the convergence of the generalized hypergeometric function.

Proof: By plugging (4) and (15) into (14), and by making some algebraic manipulations, we obtain the following equation

$$F_{\gamma_{eq}}(z) = \omega\left(1 - \Upsilon_1\left(\frac{\kappa_r}{\lambda} z^{\frac{1}{r}}\right)\right) + \frac{1-\omega}{\Gamma(\alpha)}\Upsilon_2\left(\frac{\kappa_r}{\beta} z^{\frac{1}{r}}\right) + \left(\frac{\gamma_{inc}(m, \sigma z)}{\Gamma(m)}\right)^{N_r} \begin{bmatrix} (1-\omega)\left(1 - \frac{\Upsilon_2\left(\frac{\kappa_r}{\beta} z^{\frac{1}{r}}\right)}{\Gamma(\alpha)}\right) \\ +\omega\Upsilon_1\left(\frac{\kappa_r}{\lambda} z^{\frac{1}{r}}\right) \end{bmatrix}, \tag{39}$$

where $\Upsilon_i(t)$, $i = 1, 2$ can be expressed using eqs. (07.34.03.0228.01)-(06.06.26.0004.01) of [38] as

$$\Upsilon_1(t) = G_{0,1}^{1,0}\left(t \middle| \begin{matrix} -; - \\ 0; - \end{matrix}\right), \tag{40}$$

$$\Upsilon_2(t) = G_{1,2}^{1,1}\left(t \middle| \begin{matrix} 1; - \\ \alpha; 0 \end{matrix}\right). \tag{41}$$

Then, by performing the appropriate substitutions in (21) yields

$$P_{SOP} = \frac{L\sigma_e^{m_e}}{\Gamma^L(m_e)}(D_1 + D_2 + D_3 + D_4 - D_5), \tag{42}$$

where $D_j\ (1 \le j \le 5)$ are defined as

$$D_1 = (1-\omega)\int_0^\infty \left(\frac{\gamma_{inc}(m, \sigma(2^R(z+1) - 1))}{\Gamma(m)}\right)^{N_r} \times [\gamma_{inc}(m_e, \sigma_e z)]^{L-1} e^{-\sigma_e z} z^{m_e - 1} dz, \tag{43}$$

$$D_2 = \omega\int_0^\infty \left(1 - \Upsilon_1\left(\frac{\kappa_r}{\lambda}\left(2^R(z+1) - 1\right)^{\frac{1}{r}}\right)\right) \times [\gamma_{inc}(m_e, \sigma_e z)]^{L-1} e^{-\sigma_e z} z^{m_e - 1} dz, \tag{44}$$

$$D_3 = \frac{1-\omega}{\Gamma(\alpha)}\int_0^\infty \Upsilon_2\left(\frac{\kappa_r}{\beta}\left(2^R(z+1) - 1\right)^{\frac{1}{r}}\right) \times [\gamma_{inc}(m_e, \sigma_e z)]^{L-1} e^{-\sigma_e z} z^{m_e - 1} dz, \tag{45}$$

$$D_4 = \omega\int_0^\infty \left(\frac{\gamma_{inc}(m, \sigma(2^R(z+1) - 1))}{\Gamma(m)}\right)^{N_r} e^{-\sigma_e z} \times z^{m_e - 1}\Upsilon_1\left(\frac{\kappa_r}{\lambda}\left(2^R(z+1) - 1\right)^{\frac{1}{r}}\right)[\gamma_{inc}(m_e, \sigma_e z)]^{L-1} dz, \tag{46}$$

$$D_5 = \frac{1-\omega}{\Gamma(\alpha)}\int_0^\infty \left(\frac{\gamma_{inc}(m, \sigma(2^R(z+1) - 1))}{\Gamma(m)}\right)^{N_r} e^{-\sigma_e z} \times z^{m_e - 1}[\gamma_{inc}(m_e, \sigma_e z)]^{L-1}\Upsilon_2\left(\frac{\kappa_r}{\beta}\left(2^R(z+1) - 1\right)^{\frac{1}{r}}\right) dz. \tag{47}$$

Making use of [35, Eq. (8.352.1)] alongside with the multinomial theorem, using the change of variable such as $t = 2^R z + 2^R - 1$, and with the help of the identity [38, Eq. (06.06.02.0001.01)] alongside with some algebraic manipulations, we obtain

$$D_1 = (1-\omega)\sum_{u_1=0}^{L-1}\binom{L-1}{u_1} e^{-\rho}(-1)^{u_1}\sum_{u_2=0}^{u_1}..\sum_{u_{m_e}=0}^{u_{m_e-1}}\prod_{h=0}^{m_e-1} \times \binom{u_{h+1}}{u_{h+2}}\left(\frac{1}{h!}\right)^{u_{i+1}-u_{i+2}} \sigma_e^{\delta_u}\sum_{i=0}^{\delta_u+m_e-1} \times \binom{\delta_u+m_e-1}{i}\frac{\left(1-2^R\right)^{\delta_u+m_e-1-i}}{2^{R(\delta_u+m_e)}} T_1^{(i)}, \quad (48)$$

$$D_2 = \omega\sum_{u_1=0}^{L-1}\binom{L-1}{u_1}(-1)^{u_1}\sum_{u_2=0}^{u_1}..\sum_{u_{m_e}=0}^{u_{m_e-1}}\prod_{h=0}^{m_e-1}\binom{u_{h+1}}{u_{h+2}} \times \left(\frac{1}{h!}\right)^{u_{i+1}-u_{i+2}} \sigma_e^{\delta_u} e^{-\rho}\sum_{i=0}^{\delta_u+m_e-1}\binom{\delta_u+m_e-1}{i} \times \frac{\left(1-2^R\right)^{\delta_u+m_e-1-i}}{2^{R(\delta_u+m_e)}} T_2^{(i)}, \quad (49)$$

where ρ, φ, θ_v, δ_u, and the terms $T_1^{(i)}$ and $T_2^{(i)}$ are defined in Proposition 1. In a similar manner, the remaining terms can be evaluated, which concludes the proof of Proposition 1. □

Given the incomplete Fox's H-function implementation in [37] and [39] and the SOP formula in (23), one can ascertain the practicality of this expression for exact evaluation of the considered system's SOP as a function of different values of relay antennas number, integer fading parameters, real turbulence parameters values, and average $S-R$ and $S-E$ SNRs. Furthermore, it is noteworthy that at $R=0$, this SOP formula corresponds to the intercept probability (IP) metric. Even though this formula is expressed in terms of non-elementary functions, it can be efficiently implemented in most common computing software such as Matlab or Mathematica through numerical integration over a complex contour, using the built-in "integral" or "NIntegrate" functions, respectively. For instance, the authors in [37] provided an implemented Mathematica script for computing such function. Furthermore, the analytical evaluation of this expression is significantly less complex compared to Monte Carlo simulation method. While the latter, performed on a 2.5 GHz core i7 computer, needs around two minutes per SNR value for a number of random values $N = 10^6$, the analytical evaluation's time consumption is around 15-20 seconds per SNR value, which depicts again its usefulness in terms of complexity.

4.2 Asymptotic SOP

An equivalent closed-form expression for the Incomplete Fox's H-function in (25)-(28) is given in this section, based on which, an asymptotic expansion of the derived SOP formula is provided at high SNR regime in terms of elementary functions.

4.2.1 Alternative representation

Proposition 2. *The Incomplete Fox's H-functions in (25)-(28) can be expressed as in (51) and (52), shown at the top of the next page, where $G_j^{(i)}(x,y)$ and $S_j^{(i)}(x,y)$ $(j=1,2)$ are defined as*

$$G_1^{(i)}(x,y) = \sum_{l=0}^{\infty}\frac{(-1)^l}{l!}\frac{\Gamma\left(1+i+y+\frac{l}{r}, x\left(2^R-1\right)\right)}{\left(g(x,\lambda)\right)^{-l}}, \quad (53)$$

$$G_2^{(i)}(x,y) = r\sum_{l=0}^{\infty}\frac{(-1)^l}{l!}\frac{\Gamma\left(r\left(i+y+1+l\right)\right)}{\left(g(x,\lambda)\right)^{r(i+y+1+l)}}, \quad (54)$$

$$S_1^{(i)}(x,y) = \sum_{l=0}^{\infty}\frac{(-1)^l}{l!}\Gamma\left(1+i+y+\frac{\alpha+l}{r}, x\left(2^R-1\right)\right) \times \frac{\Gamma(\alpha+l)}{\Gamma(\alpha+l+1)}\left(g(x,\beta)\right)^{\alpha+l}, \quad (55)$$

$$S_2^{(i)}(x,y) = \sum_{l=0}^{\infty}\frac{(-1)^{2r(i+y+l+1)-1}(-1)^l}{r(i+y+l+1)l!} \times \frac{\Gamma\left(\alpha+r(i+y+l+1)\right)}{\left(g(x,\beta)\right)^{r(i+y+l+1)}} + \Gamma\left(1+i+y, x\left(2^R-1\right)\right)\Gamma(\alpha), \quad (56)$$

with the couple (x,y) denotes either $(\varphi,0)$ or (ε,θ_v).

Proof: The Fox's H-function in (25) and (27) is expressed in terms of a complex integral as depicted in equation (57) at the top of the next page, where the couple (x,y)denotes either $(\varphi,0)$or (ε,θ_v).

Since the integrand function contains only simple poles of Gamma, the integral in (57) can be expressed through residues theorem as formulated in (51) [40, Theorem 1.2, Eqs. (1.2.22), (1.2.23)]. Applying this theorem, the left half plane residues can be computed as

$$G_1^{(i)}(x,y) = \sum_{l=0}^{\infty}\lim_{s\to -l}\Gamma(s)\frac{\Gamma\left(1+i+y-\frac{s}{r}, x\left(2^R-1\right)\right)}{\left(g(x,\lambda)\right)^s} \quad (59)$$

On the contrary, and as mentioned in Remark 1, the residues theorem [40, Theorem 1.2] applies only to complete Gamma functions. Thus, in order to compute the right half plane residues, we consider the particular case of Intercept probability (IP), that is $R=0$. As a result, we have

$$\Gamma\left(1+i-\frac{s}{r}, \varphi\left(2^R-1\right)\right) = \Gamma\left(1+i-\frac{s}{r}\right). \quad (60)$$

Consequently, the right poles residues can be expressed for $R=0$ as

$$G_2^{(i)}(x,y) = -\sum_{l=0}^{\infty}\lim_{s\to r(i+1+y+l)}(s-r(i+y+l+1)) \times \Gamma\left(1+y+i-\frac{s}{r}\right)\Gamma(s)\left(g(x,\lambda)\right)^{-s}. \quad (61)$$

By using the identities [40, Theorem 1.3, Eqs. (1.3.5)-(1.3.9)] and by making some algebraic manipulations, we obtain (53) and (54) which are shown in Proposition 2.

In a similar manner, the incomplete Fox's H-function in (26) and (28) given in (58) can be expressed by either the functions $S_1^{(i)}$ or $S_2^{(i)}$, representing the sum on the residues on the left and right half plane poles, respectively, as shown in (52). The integral in (58) can be computed by summing on the residues at the left half plane simple poles, that is computing on residues of $\Gamma(\alpha+s)$ using [40, Theorem 1.3, Eq. (1.3.5)] as shown in (55).

$$M_{1,1}^{1,1}\left(g(x,\lambda)\left|\begin{array}{c}(-i-y,1/r,x\left(2^R-1\right));-\\(0,1,0);-\end{array}\right.\right)=\left\{\begin{array}{l}G_1^{(i)}(x,y)\ \text{; if } (g(x,\lambda)<1 \text{ and } r=1) \text{ or } (r=2),\\ G_2^{(i)}(x,y)\ \text{; if } (g(x,\lambda)>1 \text{ and } r=1 \text{ and } R=0).\end{array}\right. \tag{51}$$

$$M_{2,2}^{1,2}\left(g(x,\beta)\left|\begin{array}{c}(-i-y,1/r,x\left(2^R-1\right)),(1,1,0);-\\(\alpha,1,0);(0,1,0)\end{array}\right.\right)=\left\{\begin{array}{l}S_1^{(i)}(x,y)\ \text{; if } (g(x,\beta)<1 \text{ and } r=1) \text{ or } (r=2),\\ S_2^{(i)}(x,y)\ \text{; if } (g(x,\beta)>1 \text{ and } r=1 \text{ and } R=0).\end{array}\right. \tag{52}$$

$$M_{1,1}^{1,1}\left(g(x,\lambda)\left|\begin{array}{c}(-i-y,1/r,x\left(2^R-1\right));-\\(0,1,0);-\end{array}\right.\right)=\frac{1}{2\pi j}\int_{\mathcal{C}}\Gamma(s)\,\Gamma\left(1+i+y-\frac{s}{r},x\left(2^R-1\right)\right)(g(x,\lambda))^{-s}\,ds. \tag{57}$$

$$M_{2,2}^{1,2}\left(g(x,\beta)\left|\begin{array}{c}(-i-y,1/r,x\left(2^R-1\right)),(1,1,0);-\\(\alpha,1,0);(0,1,0)\end{array}\right.\right)=\frac{1}{2\pi j}\int_{\mathcal{C}}\frac{\Gamma(-s)\,\Gamma\left(1+i+y-\frac{s}{r},x\left(2^R-1\right)\right)\Gamma(\alpha+s)}{\Gamma(1-s)\,(g(x,\beta))^s}ds. \tag{58}$$

Interestingly, one can notice that the Fox's H-function in (58) admits simple poles as well as double poles on the right half plane. Making use of [38, Eq. (06.05.17.0002.01)], the right half plane residues on simple poles of $\Gamma(-s)$ might be computed as [40, Theorem 1.3, Eq. (1.3.9)]

$$S_{2,0}^{(i)}(x,y)=\sum_{l=0}^{r(i+y+1)-1}\lim_{s\to l}(s-l)\frac{\Gamma(\alpha+s)}{s}\times\Gamma\left(1+i+y-\frac{s}{r},x\left(2^R-1\right)\right)(g(x,\beta))^{-s}. \tag{62}$$

We distinguish two cases

- for $l=0$:

$$\lim_{s\to 0}\Gamma\left(1+i+y-\frac{s}{r},x\left(2^R-1\right)\right)\frac{\Gamma(\alpha+s)}{(g(x,\beta))^s}=\Gamma\left(1+i+y,x\left(2^R-1\right)\right)\Gamma(\alpha). \tag{63}$$

- for $l>0$:

$$\sum_{l=1}^{r(i+y+1)-1}\lim_{s\to l}\frac{(s-l)}{s}\Gamma\left(1+i+y-\frac{s}{r},x\left(2^R-1\right)\right)\times\Gamma(\alpha+s)(g(x,\beta))^{-s}=0. \tag{64}$$

Consequently, the function defined in (62) is expressed as

$$S_{2,0}^{(i)}(x,y)=\Gamma\left(1+i+y,x\left(2^R-1\right)\right)\Gamma(\alpha). \tag{65}$$

The integrand function (58) admits also double poles of $\Gamma(-s)$ and $\Gamma\left(1+i-\frac{s}{r},\varphi\left(2^R-1\right)\right)$. As discussed in Remark 1, and similarly to the simple poles case, the residues theorem for poles of order $N\geq 1$ applies only for complete Gamma functions. That is, we consider the case of $R=0$ (IP).

Using [40, Theorem 1.4, Eq. (1.4.2)], the residues at poles of order $N=2$ are calculated as

$$-\sum_{l=0}^{\infty}\lim_{s\to r(i+y+l+1)}Q^{(i)}(s,x,y), \tag{66}$$

with

$$Q^{(i)}(s,x,y)=\left(H_1^{(i)}(s,x,y)H_2^{(i)}(s,x,y)z^{-s}\right)', \tag{67}$$

$$H_1^{(i)}(s,x,y)=(s-r(i+y+l+1))^2\Gamma(-s)\times\Gamma\left(1+i+y-\frac{s}{r}\right), \tag{68}$$

$$H_2^{(i)}(s)=\frac{\Gamma(\alpha+s)}{\Gamma(1-s)}. \tag{69}$$

By carrying out some algebraic manipulations, we obtain

$$Q^{(i)}(s,x,y)=(g(x,\beta))^{-s}\times\left[\begin{array}{c}(s-r(i+y+l+1))^2\Gamma\left(1+i+y-\frac{s}{r}\right)\\ \times\frac{\Gamma(-s)\Gamma(\alpha+s)[-\ln(g(x,\beta))+\Psi(\alpha+s)+\Psi(1-s)]}{\Gamma(1-s)}\\ +(s-r(i+y+l+1))\Gamma(-s)\,\Gamma\left(1+i+y-\frac{s}{r}\right)\\ \times\frac{\Gamma(\alpha+s)}{\Gamma(1-s)}\left(\begin{array}{c}2-(s-r(i+y+l+1))\\ \times\left[\Psi(-s)+\frac{1}{r}\Psi(1+i+y-\frac{s}{r})\right]\end{array}\right)\end{array}\right]. \tag{70}$$

By taking the first term of (70), we have

$$S_{2,1}^{(i)}(x,y)=-\sum_{l=0}^{\infty}\lim_{s\to r(i+y+l+1)}(s-r(i+y+l+1))^2\Gamma(-s)\times\frac{\Gamma(\alpha+s)\left[-\ln(g(x,\beta))+\Psi(\alpha+s)+\Psi(1-s)\right]}{\Gamma(1-s)}\times\Gamma\left(1+y+i-\frac{s}{r}\right). \tag{71}$$

By putting the following change of variable $s\to r(i+y+l+1)-\varepsilon\Leftrightarrow 1-s\to 1-r(i+y+l+1)+\varepsilon$, with $\varepsilon\to 0$, we obtain

$$S_{2,1}^{(i)}(x,y)=-\sum_{l=0}^{\infty}\lim_{\varepsilon\to 0}\varepsilon^2\Gamma(-r(i+y+l+1)+\varepsilon)\,\Gamma\left(-l+\frac{\varepsilon}{r}\right)\times W^{(i)}(s,x,y)(g(x,\beta))^{-r(i+y+l+1)+\varepsilon}, \tag{72}$$

where $W^{(i)}(s,x,y)$ is given as

$$W^{(i)}(s,x,y)=\frac{\Gamma(\alpha+r(i+y+l+1)-\varepsilon)}{\Gamma(1-r(i+y+l+1)+\varepsilon)}\times\left[\begin{array}{c}\Psi(\alpha+r(i+y+l+1)-\varepsilon)\\ +\Psi(1-r(i+y+l+1)+\varepsilon)\\ -\ln(g(x,\beta))\end{array}\right]. \tag{73}$$

By using eqs. (06.14.06.0024.01) and (06.05.17.0003.01)] of [38], and [40, Theorem 1.3, Eq. (1.3.9)], and after some

algebraic manipulations, we obtain the equation (74) at the top of this next page.

Similarly, the second term is calculated as

$$S_{2,2}^{(i)}(x,y) = -\sum_{l=0}^{\infty} \lim_{\varepsilon\to 0} \varepsilon\Gamma\left(-r(i+y+l+1)+\varepsilon\right)\Gamma\left(-l+\frac{\varepsilon}{r}\right) \times \frac{\left[2-\varepsilon\left[\Psi(-r(i+y+l+1)+\varepsilon)+\frac{1}{r}\Psi(-l+\frac{\varepsilon}{r})\right]\right]}{\Gamma\left(1-r(i+y+l+1)+\varepsilon\right)} \times \frac{\Gamma\left(\alpha+r(i+y+l+1)-\varepsilon\right)}{\left(g(x,\beta)\right)^{r(i+y+l+1)+\varepsilon}}. \quad (75)$$

Involving eqs. (06.14.06.0024.01) and (06.05.17.0003.01) of [38] into (75) yields

$$S_{2,2}^{(i)}(x,y) = -\sum_{l=0}^{\infty} \lim_{\varepsilon\to 0} \varepsilon\Gamma\left(-r(i+y+l+1)+\varepsilon\right)\Gamma\left(-l+\frac{\varepsilon}{r}\right) \times \left(1-r(i+y+l+1)+\varepsilon\right)_{r(i+y+l+1)} \times \frac{\varepsilon\left[\Psi(r(i+y+l+1))+\frac{1}{r}\Psi(l+1)\right]}{\Gamma\left(1+\varepsilon\right)} \times \frac{\Gamma\left(\alpha+r(i+y+l+1)-\varepsilon\right)}{\left(g(x,\beta)\right)^{r(i+y+l+1)-\varepsilon}} = 0. \quad (76)$$

where $(a)_n$ denotes the Pochhammer symbol [38, Eq. (06.10.02.0001.01)]. Finally, by summing up the terms $S_{2,0}^{(i)}(x,y)$, $S_{2,1}^{(i)}(x,y)$, and $S_{2,2}^{(i)}(x,y)$, given in (65), (74), and (76), respectively, $S_2^{(i)}(x,y)$ is expressed as

$$S_2^{(i)}(x,y) = \sum_{l=0}^{\infty} \frac{(-1)^{2r(i+y+l+1)-1}(-1)^l}{\left(g(x,\beta)\right)^{r(i+y+l+1)}\left(r(i+y+l+1)l!\right.} \times \Gamma\left(\alpha+r(i+y+l+1)\right) + \Gamma\left(\alpha\right)\Gamma\left(1+i+y,\varphi\left(2^R-1\right)\right), \quad (77)$$

which concludes the result provided in Proposition 2. □

Remark 1. *Thus, equations (51)-(56) depict an alternative analytical closed-form expressions of the incomplete Fox's H-functions given in (23). These expressions are calculated based on the residues theorem, where the Fox's H-function equals either the sum on the residues of the left half plane poles or right half plane ones, depending on the value of its argument (e.g, $z = \frac{\kappa}{t}x^{-\frac{1}{r}}$), defined in (37), with t equals either λ or β.*

From another front, it is worth noting that the computation on left half plane through residues theorem can be applied when the conditions $\frac{\kappa}{t}x^{-\frac{1}{r}} < 1$ and $r = 1$ (i.e., coherent detection), or $r = 2$ (i.e., IM/DD) are satisfied. However, when $\frac{\kappa}{t}x^{-\frac{1}{r}} > 1$ and $r = 1$, the residues theorem [40, Theorem 1.2] does not apply straightforwardly for the incomplete Gamma function (e.g., $\Gamma\left(1+i+y-\frac{s}{r},x\left(2^R-1\right)\right)$. Given this fact, the computation in the right half plane through the abovementioned theorem will be restricted in this paper only for the complete Gamma function (i.e., $R = 0$). That is only Intercept Probability expression can be computed in this regard.

4.2.2 Asymptotic expression

Corollary 1. *The asymptotic expansion of the secrecy outage probability expression at high average SNR values, when $\mu_r = \xi\overline{\gamma}$, with $\xi > 0$, is given as*

$$P_{sop}^{\infty} \sim \frac{L\sigma_e^{m_e}}{\Gamma^L\left(m_e\right)} B_2 \overline{\gamma}^{-\frac{1}{r}}, \quad (78)$$

where

$$B_2 = \omega\frac{\mathbb{E}\left[I\right]}{\lambda}\xi^{-\frac{1}{r}}\left(\Gamma\left(m_e\right)\right)^{L-1}\sum_{u_1=0}^{L-1}\binom{L-1}{u_1}(-1)^{u_1} \times \sum_{u_2=0}^{u_1}\cdots\sum_{u_{m_e}=0}^{u_{m_e-1}}\prod_{h=0}^{m_e-1}\binom{u_{h+1}}{u_{h+2}}\left(\frac{1}{h!}\right)^{u_{i+1}-u_{i+2}}\sigma_e^{\delta_u}e^{-\rho} \times \sum_{p=0}^{\delta_u+m_e-1}\binom{\delta_u+m_e-1}{p}\frac{\left(1-2^R\right)^{\delta_u+m_e-1-p}}{\varphi^{p+\frac{1}{r}+1}2^{R(\delta_u+m_e)}} \times \Gamma\left(p+\frac{1}{r}+1,\varphi\left(2^R-1\right)\right). \quad (79)$$

Remark 2. *From (78), one can notice evidently that the achievable diversity order of the SOP expression is $G_d = \frac{1}{r}$.*

Proof: Each term D_k, $k = 1,..,5$, given in (43)-(47), can be asymptotically written as

$$D_k \sim A_k + \frac{B_k}{\overline{\gamma}^{C_k}}, k = 1,..5, \quad (80)$$

where C_k denotes the asymptotic order of the term.

- Term D_1 :
  One can notice that A_k can be obtained by computing $\lim_{\overline{\gamma}\to\infty} D_k$. So, to compute the abovementioned three constants, it is sufficient to evaluate the limit $\lim_{\overline{\gamma}\to\infty} D_k\overline{\gamma}^i$, for $i = 0$, C_k.

By computing the limit of the term $D_1\overline{\gamma}^i$, with $i > 0$ and D_1 given in (43), when $\overline{\gamma}\to\infty$, one obtains

$$\lim_{\overline{\gamma}\to\infty} D_1\overline{\gamma}^i = (1-\omega)\int_0^{\infty}\left[\gamma_{inc}\left(m_e,\sigma_e z\right)\right]^{L-1}e^{-\sigma_e z}z^{m_e-1} \times \lim_{\overline{\gamma}\to\infty}\left\{\left(\frac{\gamma_{inc}\left(m,\frac{m\left(2^R(z+1)-1\right)}{\overline{\gamma}}\right)}{\Gamma\left(m\right)}\right)^{N_r}\overline{\gamma}^i\right\}dz. \quad (81)$$

As $\gamma_{inc}\left(m,x\right)$ approximately equals x^m near $x = 0$, it follows that

$$\lim_{\overline{\gamma}\to\infty} D_1\overline{\gamma}^i = \begin{cases} 0; \text{ if } i < mN_r \\ B_1; \text{ if } i = mN_r \\ \infty; \text{ if } i > mN_r \end{cases} \quad (82)$$

where

$$B_1 = \frac{m^{mN_r}(1-\omega)}{\Gamma^{N_r}\left(m\right)}\int_0^{\infty}\left(2^R(z+1)-1\right)^{mN_r}e^{-\sigma_e z}z^{m_e-1} \times \left[\gamma_{inc}\left(m_e,\sigma_e z\right)\right]^{L-1}dz. \quad (83)$$

Consequently, in high SNR regime (i.e., $\overline{\gamma}\to\infty$), D_1 can be asymptotically expressed as

$$S_{2,1}^{(i)}(x,y) = -\sum_{l=0}^{\infty} \lim_{\varepsilon\to 0} \frac{(-1)^{r(i+y+l+1)}(-1)^{l}}{(r(i+y+l+1))!l!}\Gamma\left(\alpha + r(i+y+l+1)\right)(-1)^{r(i+y+l+1)-1}(r(i+y+l+1)-1)!\varepsilon$$
$$\times \frac{\left[\ln\left(g(x,\beta)\right) + \Psi\left(\alpha+s\right) - \frac{1}{\varepsilon} + \Psi\left(r(i+y+l+1)\right)\right]}{\Gamma\left(1+\varepsilon\right)}\left(g(x,\beta)\right)^{-r(i+y+l+1)+\varepsilon},$$
$$= \sum_{l=0}^{\infty} \frac{(-1)^{2r(i+y+l+1)-1}(-1)^{l}}{(r(i+y+l+1)l!}\Gamma\left(\alpha + r(i+y+l+1)\right)\left(g(x,\beta)\right)^{-r(i+y+l+1)}. \quad (74)$$

$$D_1 \sim B_1 \overline{\gamma}^{-mN_r}. \quad (84)$$

- Term D_2 :
The limit of $D_2\overline{\gamma}^i$, with D_2 given in (44), when $\overline{\gamma}\to\infty$ can be expressed as

$$\lim_{\overline{\gamma}\to\infty} D_2\overline{\gamma}^i = \omega\int_0^{\infty}\left[\gamma_{inc}\left(m_e,\sigma_e z\right)\right]^{L-1} e^{-\sigma_e z} z^{m_e-1}dz$$
$$\times \lim_{\overline{\gamma}\to\infty}\left(1-\Upsilon_1\left(\tfrac{\kappa_r}{\lambda}\left(2^R(z+1)-1\right)^{\frac{1}{r}}\right)\right)$$
$$\times\,\overline{\gamma}^i. \quad (85)$$

where

$$\Upsilon_1\left(t\right) = \exp\left(-t\right). \quad (86)$$

At high SNR values, $\exp(-x)$ approximately equals $1-x$. It follows that equation (85) can be written as

$$\lim_{\overline{\gamma}\to\infty} D_2\overline{\gamma}^i = \omega\lim_{\overline{\gamma}\to\infty}\left\{\overline{\gamma}^{i-\frac{1}{r}}\frac{\mathbb{E}\left[I\right]}{\lambda}\xi^{-\frac{1}{r}}\right\}\int_0^{\infty} e^{-\sigma_e z} z^{m_e-1}$$
$$\times\left[\gamma_{inc}\left(m_e,\sigma_e z\right)\right]^{L-1}\left(2^R(z+1)-1\right)^{\frac{1}{r}}dz, \quad (87)$$

or equivalently to

$$\lim_{\overline{\gamma}\to\infty} D_2\overline{\gamma}^i = \begin{cases} 0; \text{ if } i<\frac{1}{r} \\ B_2; \text{ if } i=\frac{1}{r} \\ \infty; \text{ if } i>\frac{1}{r} \end{cases} \quad (88)$$

Consequently, D_2 is asymptotically expressed at high SNR as

$$D_2 = B_2\overline{\gamma}^{-\frac{1}{r}}, \quad (89)$$

with

$$B_2 = \frac{\omega\mathbb{E}\left[I\right]}{\lambda}\xi^{-\frac{1}{r}}\int_0^{\infty}\left(2^R(z+1)-1\right)^{\frac{1}{r}}$$
$$\times\int_0^{\infty}\left[\gamma_{inc}\left(m_e,\sigma_e z\right)\right]^{L-1} e^{-\sigma_e z} z^{m_e-1}dz. \quad (90)$$

Using the change of variable such as $t = 2^R z + 2^R - 1$, and with the help of the identity [38, Eq. (06.06.02.0001.01)] alongside with some algebraic manipulations, (79) is attained.

- Term D_3 :
The limit of $D_3\overline{\gamma}^i$, with D_2 given in (45), when $\overline{\gamma}\to\infty$ can be expressed as

$$\lim_{\overline{\gamma}\to\infty} D_3\overline{\gamma}^i = \frac{1-\omega}{\Gamma\left(\alpha\right)}\int_0^{\infty}\left[\gamma_{inc}\left(m_e,\sigma_e z\right)\right]^{L-1}\frac{z^{m_e-1}}{e^{\sigma_e z}}dz$$
$$\times\lim_{\overline{\gamma}\to\infty}\left\{\Upsilon_2\left(\frac{\kappa_r}{\beta}\left(2^R(z+1)-1\right)^{\frac{1}{r}}\right)\overline{\gamma}^i\right\}. \quad (91)$$

where

$$\Upsilon_2\left(t\right) = \gamma_{inc}\left(\alpha,t\right). \quad (92)$$

At high SNR values, it follows that equation (91) can be written as

$$\lim_{\overline{\gamma}\to\infty} D_3\overline{\gamma}^i = \epsilon\lim_{\overline{\gamma}\to\infty}\left\{\overline{\gamma}^{i-\frac{\alpha}{r}}\left(2^R(z+1)-1\right)^{\frac{\alpha}{r}}\right\}$$
$$\times\int_0^{\infty}\left[\gamma_{inc}\left(m_e,\sigma_e z\right)\right]^{L-1} e^{-\sigma_e z} z^{m_e-1}dz, \quad (93)$$

with $\epsilon = \frac{1-\omega}{\Gamma(\alpha)}\left(\frac{\mathbb{E}[I]}{\beta}\xi^{-\frac{1}{r}}\right)^{\alpha}$, or equivalently to

$$\lim_{\overline{\gamma}\to\infty} D_3\overline{\gamma}^i = \begin{cases} 0; \text{ if } i<\frac{\alpha}{r} \\ B_3; \text{ if } i=\frac{\alpha}{r} \\ \infty; \text{ if } i>\frac{\alpha}{r} \end{cases} \quad (94)$$

with

$$B_3 = \epsilon\int_0^{\infty}\left(2^R(z+1)-1\right)^{\frac{\alpha}{r}}\left[\gamma_{inc}\left(m_e,\sigma_e z\right)\right]^{L-1}$$
$$\times\, e^{-\sigma_e z} z^{m_e-1}dz. \quad (95)$$

Consequently, D_3 is asymptotically expressed at high NR Sas

$$D_3 = B_3\overline{\gamma}^{-\frac{\alpha}{r}}. \quad (96)$$

- Term D_4 :
In a similar manner, the limit of $D_4\overline{\gamma}^i$, with D_4 given in (46), when $\overline{\gamma}\to\infty$ can be expressed as

$$\lim_{\overline{\gamma}\to\infty} D_4\overline{\gamma}^i = \omega\int_0^{\infty} e^{-\sigma_e z} z^{m_e-1}\left[\gamma_{inc}\left(m_e,\sigma_e z\right)\right]^{L-1}dz$$
$$\times\lim_{\overline{\gamma}\to\infty}\left\{\begin{array}{c}\overline{\gamma}^i\left(\frac{\gamma_{inc}\left(m,\frac{m}{\overline{\gamma}}\left(2^R(z+1)-1\right)\right)}{\Gamma(m)}\right)^{N_r} \\ \times\Upsilon_1\left(\frac{\kappa_r}{\lambda}\left(2^R(z+1)-1\right)^{\frac{1}{r}}\right)\end{array}\right\}. \quad (97)$$

It follows that for high SNR values, (97) can be written as

$$\lim_{\overline{\gamma}\to\infty} D_4\overline{\gamma}^i = \omega \int_0^\infty \left[\gamma_{inc}\left(m_e, \sigma_e z\right)\right]^{L-1} e^{-\sigma_e z} z^{m_e-1} \times \lim_{\overline{\gamma}\to\infty} \left\{ \left(\frac{\gamma_{inc}\left(m, \frac{m\left(2^R(z+1)-1\right)}{\overline{\gamma}}\right)}{\Gamma\left(m\right)} \right)^{N_r} \overline{\gamma}^i \right\} dz, \tag{98}$$

or equivalently to

$$\lim_{\overline{\gamma}\to\infty} D_4\overline{\gamma}^i = \begin{cases} 0; \text{ if } i < mN_r \\ \frac{\omega}{1-\omega} B_1; \text{ if } i = mN_r \\ \infty; \text{ if } i > mN_r \end{cases} \tag{99}$$

That is, for high SNR values, D_4 can be approximately expressed as

$$D_4 \sim \frac{\omega}{1-\omega} B_1 \overline{\gamma}^{-mN_r}. \tag{100}$$

- Term D_5 :

In a similar manner, the limit of $D_5\overline{\gamma}^i$ when $\overline{\gamma} \to \infty$ can be expressed as

$$\lim_{\overline{\gamma}\to\infty} D_5\overline{\gamma}^i = \omega \int_0^\infty e^{-\sigma_e z} z^{m_e-1} \left[\gamma_{inc}\left(m_e, \sigma_e z\right)\right]^{L-1} dz \times \lim_{\overline{\gamma}\to\infty} \left\{ \begin{array}{l} \left(\frac{\gamma_{inc}\left(m, \frac{m\left(2^R(z+1)-1\right)}{\overline{\gamma}}\right)}{\Gamma(m)} \right)^{N_r} \\ \times \Upsilon_2\left(\frac{\kappa_r}{\beta}\left(2^R(z+1)-1\right)^{\frac{1}{r}}\right) \overline{\gamma}^i \end{array} \right\} dz. \tag{101}$$

At high SNR values, we have

$$\lim_{\overline{\gamma}\to\infty} D_5\overline{\gamma}^i = \epsilon \frac{m^{mN_r}}{\Gamma^{N_r}\left(m\right)} \lim_{\overline{\gamma}\to\infty} \overline{\gamma}^{i-\frac{\alpha}{r}-mN_r} \times \int_0^\infty \left(2^R(z+1)-1\right)^{mN_r+\frac{\alpha}{r}} e^{-\sigma_e z} z^{m_e-1} \times \left[\gamma_{inc}\left(m_e, \sigma_e z\right)\right]^{L-1} dz. \tag{102}$$

Or equivalently

$$\lim_{\overline{\gamma}\to\infty} D_5\overline{\gamma}^i = \begin{cases} 0; \text{ if } i < mN_r \\ B_5; \text{ if } i = mN_r \\ \infty; \text{ if } i > mN_r \end{cases} \tag{103}$$

with

$$B_5 = \epsilon \frac{m^{mN_r}}{\Gamma^{N_r}\left(m\right)} \int_0^\infty \left[\gamma_{inc}\left(m_e, \sigma_e z\right)\right]^{L-1} \times \left(2^R(z+1)-1\right)^{mN_r+\frac{\alpha}{r}} e^{-\sigma_e z} z^{m_e-1} dz.$$

From the above, one can notice clearly that the asymptotic order of the terms D_i, $1 \le i \le 5$, equals mN_r, $\frac{1}{r}$, $\frac{\alpha}{r}$, $\frac{1}{r}+mN_r$, and $\frac{\alpha}{r}+mN_r$, respectively. Given that $mN_r \ge 1$, $\alpha > 1$ [8], and r equals either 1 or 2, the terms D_1, D_3, D_4, and D_5 will be neglected compared to D_2 as it is the term with least order, that is $\frac{1}{r}$. Consequently, the achievable diversity order is $G_d = \frac{1}{r}$. □

5 Numerical Results

The derived analytic results, which are corroborated with respective Monte Carlo results, are employed in this section to analyze the performance of the considered set up. Some illustrative numerical examples are depicted to examine the effects of the key system parameters on the overall secrecy performance of the considered mixed RF/UOWC system. To this end, the system and channel parameters are set as $m = m_e = 2$ for the $S-R$ and $S-E$ links fading severity, $\overline{\gamma}_e = \{0 \text{ dB}, 5 \text{ dB}, 10 \text{ dB}\}$, and $L = \{1, 2, 3\}$ denotes the number of eavesdroppers for the wiretap link, while the number of antennas at the relay is considered as $N_r = \{1, 2, 3\}$, and $\alpha = 6.7615, \beta = 0.3059, \lambda = 0.1992$, $\omega = 0.5717$, and $\eta = 0.7$ for the $R-D$ link turbulence severity. In addition, the simulation is performed by generating 5×10^5 random samples, while we fixed the threshold rate to $R = 1$ bps/Hz.

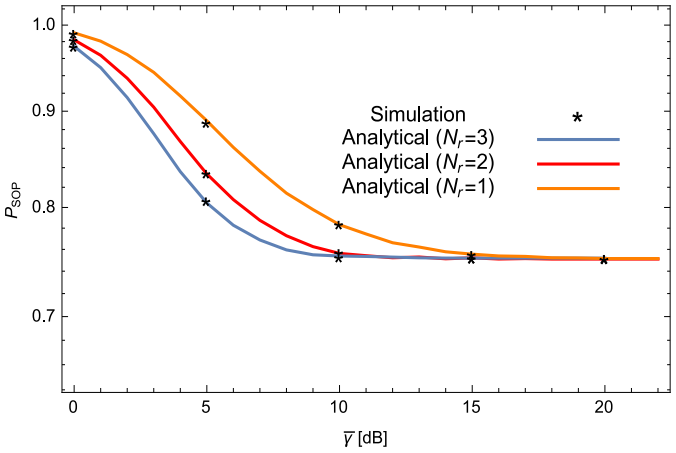

Fig. 2: SOP of the mixed RF/UOWC system versus average S-R SNR for coherent detection.

Fig. 2 shows the SOP given in (23) as a function of the S-R average SNR per branch $\overline{\gamma}$. The average R-D SNR is fixed to $\mu_r = 3$ dB, the number of eavesdroppers to $L = 2$, and eavesdropper's average SNR $\overline{\gamma}_e = 0$ dB. Furthermore, relay's receive antennas number is varied and coherent detection technique is assumed. One can ascertain obviously from the figure that the analytical curves match with the simulation results in starred markers. From another front, we notice that the system's SOP decreases as a function of $\overline{\gamma}$, for a fixed number of relay antennas N_r and eavesdroppers' received SNR $\overline{\gamma}_e$. Actually, increasing the legitimate link's SNR $\overline{\gamma}$ while keeping the wiretap link SNR $\overline{\gamma}_e$ fixed, results in increasing the main link's capacity, and consequently the secrecy capacity increases. As a result, this increasing capacity will most unlikely fall below a certain threshold R, achieving a better secrecy performance. For example, the greater is the number of receive antennas N_r, the higher is the average secrecy capacity, and consequently the more reliable is the wireless communication.

In Figs. 3 and 4, the impact of the detection technique type, the eavesdropper's received SNR, as well as the number of eavesdropping nodes L on the system's SOP performance is illustrated. It can be clearly noticed in Fig. 3 that the system's secrecy outage performance deteriorates in the

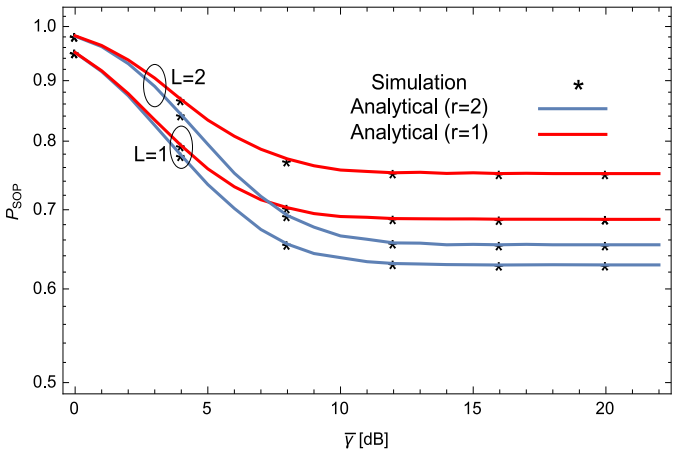

Fig. 3: SOP of the mixed RF/UOWC system versus average S-R SNR.

case of coherent technique, compared to IM/DD detection. In fact, IM/DD technique is the simplest and widely used technique, since it is based on amplifying the incoming light intensity and then demodulating it, while coherent detection is based on restoring the wave's carrier phase [41]. Consequently, in addition to its complexity, coherent technique results also in a worse secrecy performance compared to its IM/DD counterpart. On the other hand, it is clearly observed that the SOP curves admit a certain limit at high SNR regime, where the curves justify to a certain limit value despite increasing $\overline{\gamma}$ and N_r values. This is due to the fact that at higher $\overline{\gamma}$ values (e.g., $\gamma_{SR} \to \infty$) or greater number of relay antennas values (N_r), the end-to-end SNR at the destination, given in (13) as the minimum of γ_{SR} and R-D SNR γ_{RD}, will be always equal to γ_{RD}, and consequently, the system's secrecy performance is dominated by the worst hop, that is R-D. Furthermore, one can notice also the impact of the number of eavesdroppers L. The higher L is, the greater is the SOP, and consequently, the secrecy performance of the system deteriorates.

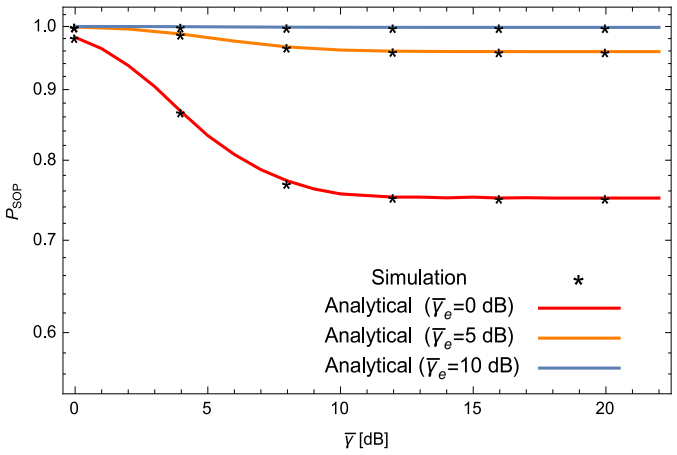

Fig. 4: SOP of the mixed RF/UOWC system versus average S-R SNR for coherent detection.

It is also noticed in Fig. 4 the impact of varying S-E average SNR ($\overline{\gamma}_e$) on the SOP for a fixed legitimate link SNR. For instance, the secrecy performance of the system for an SNR per eavesdropper $\overline{\gamma}_e = 10$ dB is worse than the cases of lower eavesdropper SNR, that are $\overline{\gamma}_e = 5$ dB and $\overline{\gamma}_e = 0$ dB, respectively. Thus, the more powerful is the wiretap link in terms of nodes' number (greater L) and/or eavesdroppers received signal power, the greater is the wiretap link capacity, and consequently, the more likely the legitimate communication is overheard.

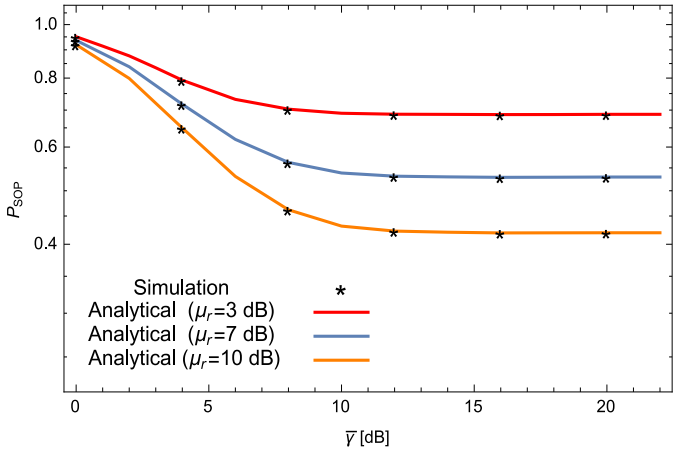

Fig. 5: SOP of the mixed RF/UOWC system versus average S-R SNR for coherent detection and different μ_r values.

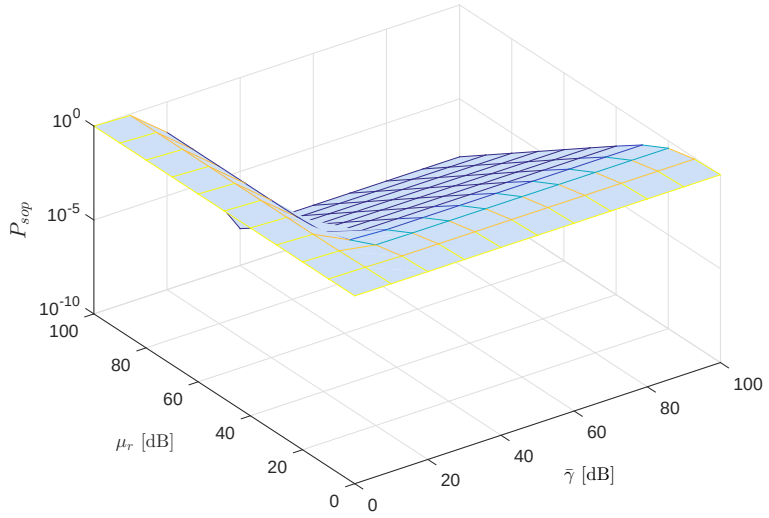

Fig. 6: SOP of the mixed RF/UOWC system versus $\overline{\gamma}$ and μ_r.

Fig. 5 and Fig. 6 show the SOP evolution versus both hops SNRs ($\overline{\gamma}$ and μ_r), in 2D and 3D, respectively. It is obviously seen that the greater the R-D average SNR (μ_r) is, the lower is the SOP value, and consequently, the better is the achievable secrecy performance. Moreover, similarly to previous figures, we can clearly ascertain that the SOP admits a limit at higher μ_r values, that is $\mu_r \to \infty$, where the secrecy performance of the system remains steady. As mentioned above, since from (13) that the total SNR is the minimum of γ_{SR} and γ_{RD}, despite increasing μ_r to higher

values, the system's secrecy performance is dominated by the worst hop, that is S-R in this case.

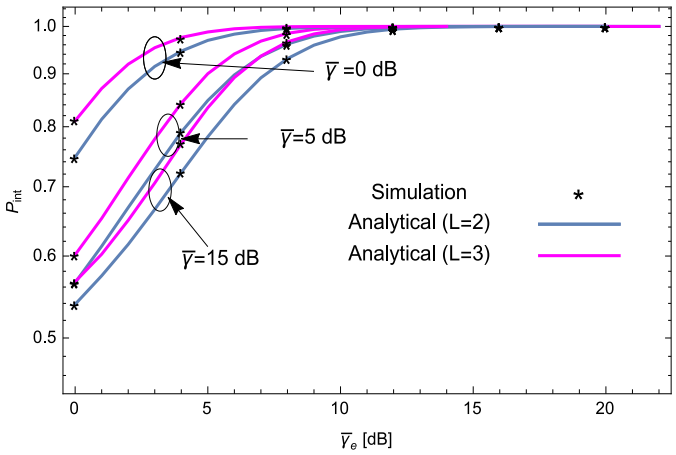

Fig. 7: Intercept probability of the mixed RF/UOWC system versus average S-E SNR for coherent detection and different L values.

Fig. 7 depicts the intercept probability (IP) metric, which is the SOP evaluated at a threshold rate $R = 0$, versus S-E SNR $\overline{\gamma}_e$ for $L = 2, 3$ as the number of eavesdroppers. In fact, IP depicts the scenario where the main link capacity is less than that of the wiretap channel. In fact, from the SOP definition provided in (16), one can obviously notice that the greater the threshold rate R is, the higher is the SOP. Consequently, the system's security becomes less reliable. As discussed in the previous figure, it can be clearly viewed that the intercept probability increases as a function of the wiretap channel SNR $\overline{\gamma}_e$, and the number of eavesdropping nodes. In fact, the more dominant the wiretap link is, in terms of number of wiretappers (higher L) and/or eavesdroppers received signal power, the greater is the wiretap link capacity, and consequently, it is more likely that the legitimate communication is overheard. In addition, we ascertain that the 2 curves' cluster on the right corresponding to an S-R SNR of 15 dB shows a better secrecy performance compared to other clusters (e.g., 0 dB, and 5 dB cases), thus, it corroborates again that a higher transmit power impacts positively the communication reliability. Furthermore, one can notice also that for higher values of $\overline{\gamma}_e$ (e.g., $\overline{\gamma}_e \to \infty$), the IP tends to be 1, that is a certain eavesdropping scenario. Also, the wiretap link capacity will certainly surpass the main link's one when the wiretap link average SNR $\overline{\gamma}_e$ exceeds a certain threshold, that is IP tends to 1.

Fig. 8 depicts the SOP versus $\overline{\gamma}$ alongside with the corresponding asymptotic result in (78) for varying μ_r values, $\overline{\gamma}_e = 10$ dB, $m = 2$, $N_r = 2$, and considering both detection techniques. In particular, we depict three scenarios, namely $\mu_r = \overline{\gamma}$, $\mu_r = 2\overline{\gamma}$, and $\mu_r = \frac{\overline{\gamma}}{2}$. Distinctly from previous figures, it can be remarkably seen that the higher the average R-D SNR (μ_r) is, the greater is the secrecy capacity, and consequently, the SOP tends to zero at higher SNR values. Furthermore, the results shows that the asymptotic SOP curves converge to the respective exact derived results at high SNR regime.

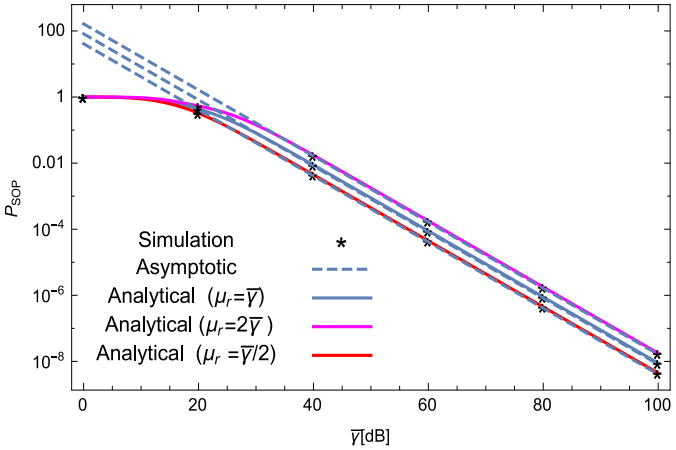

Fig. 8: SOP of the mixed RF/UOWC system versus $\overline{\gamma}$ for $\overline{\gamma}_e = 10$ dB.

6 Conclusion

The secrecy outage probability of a dual-hop DF mixed RF/UOWC system is investigated in this work. An exact closed-form expression for the secrecy outage probability is derived, in terms of the incomplete Fox's H-function, based on which the impact of key system parameters on the overall secrecy performance was investigated. In addition, we provided an alternative expression of the derived SOP metric by invoking the residues theorem to express the hypergeometric incomplete Fox's H-function through the sum of residues, in terms of elementary functions. Based on this result, an asymptotic analysis of the SOP expression at high SNR regime is performed.

It is shown that the secrecy performance of the system improves significantly by increasing the legitimate link parameters (i.e., average S and R transmit powers (i.e., average S-R and R-D SNRs) and the number of relay antennas). However, the secrecy performance get worse when the wiretap link is dominating in terms of received SNR and/or number of eavesdroppers L. Moreover, the asymptotic behavior of the SOP metric shows that at high $S - R$ average SNR, the system's secrecy outage performance is dominated only by the R-D link despite increasing S-R link parameters, such as the number of relay antennas and the average received SNR at the relay branches. It is shown also that varying R-D average SNR with respect to the S-R one yields a better secrecy performance, compared to the case of fixing it to a certain value, that is resulting in steady secrecy performance. Moreover, the achieved diversity order equals $1/r$, despite the value of the fading parameter m or the number of antennas at the relay.

A potential extension of this work is the consideration of multiple source nodes equipped with multiple antennas. In addition, the consideration of friendly jammers and/or artificial noise to increase security arise as an interesting issue to be investigated. This is expected to give useful insights on the computational requirements and sustainability of practical deployments.

REFERENCES

[1] Y. R. Ortega, P. K. Upadhyay, D. B. da Costa, P. S. Bithas, A. G. Kanatas, U. S. Dias, and R. T. de Sousa Junior, "Joint effect of jamming and noise in wiretap channels with multiple antennas," in *2017 13th International Wireless Communications and Mobile Computing Conference (IWCMC)*, June 2017, pp. 1344–1349.

[2] M. Bloch, J. Barros, M. R. D. Rodrigues, and S. W. McLaughlin, "Wireless Information-Theoretic Security," *IEEE Trans. Inf. Theory*, vol. 54, no. 6, pp. 2515–2534, June 2008.

[3] A. D. Wyner, "The wire-tap channel," *The Bell System Technical Journal*, vol. 54, no. 8, pp. 1355–1387, Oct 1975.

[4] L. Fan, X. Lei, N. Yang, T. Q. Duong, and G. K. Karagiannidis, "Secure Multiple Amplify-and-Forward Relaying With Cochannel Interference," *IEEE Journal of Selected Topics in Signal Processing*, vol. 10, no. 8, pp. 1494–1505, Dec 2016.

[5] M. Bouabdellah, F. E. Bouanani, and H. Ben-azza, "Secrecy outage probability in cognitive radio networks subject to Rayleigh fading channels," in *2018 International Conference on Advanced Communication Technologies and Networking (CommNet)*, April 2018, pp. 1–5.

[6] L. Kong and G. Kaddoum, "On Physical Layer Security Over the Fisher-Snedecor $\mathcal{F}$ Wiretap Fading Channels," *IEEE Access*, vol. 6, pp. 39 466–39 472, 2018.

[7] Z. Zeng, S. Fu, H. Zhang, Y. Dong, and J. Cheng, "A Survey of Underwater Optical Wireless Communications," *IEEE Commun. Surveys Tuts.*, vol. 19, no. 1, pp. 204–238, First quarter 2017.

[8] E. Zedini, H. M. Oubei, A. Kammoun, M. Hamdi, B. S. Ooi, and M. S. Alouini, "A New Simple Model for Underwater Wireless Optical Channels in the Presence of Air Bubbles," in *GLOBECOM 2017 - 2017 IEEE Global Communications Conference*, Dec 2017, pp. 1–6.

[9] H. Kaushal and G. Kaddoum, "Underwater Optical Wireless Communication," *IEEE Access*, vol. 4, pp. 1518–1547, 2016.

[10] S. Arnon, J. Barry, G. Karagiannidis, R. Schober, and M. Uysal, *Advanced Optical Wireless Communication Systems*. The Edinburgh Building, Cambridge CB2 8RU, UK: Cambridge University Press, 2012.

[11] I. S. Ansari, "On the Performance of Free-Space Optical Systems over Generalized Atmospheric Turbulence Channels with Pointing Errors," Ph.D. dissertation, King Abdullah University of Science and Technology (KAUST), Thuwal, Makkah Province, Kingdom of Saudi Arabia, February 2015.

[12] M. O. Hasna and M. S. Alouini, "A performance study of dual-hop transmissions with fixed gain relays," *IEEE Trans. Wireless Commun.*, vol. 3, no. 6, pp. 1963–1968, Nov 2004.

[13] X. Bao and J. Li, "Efficient Message Relaying for Wireless User Cooperation: Decode-Amplify-Forward (DAF) and Hybrid DAF and Coded-Cooperation," *IEEE Transactions on Wireless Communications*, vol. 6, no. 11, pp. 3975–3984, November 2007.

[14] J. He, V. Tervo, X. Zhou, X. He, S. Qian, M. Cheng, M. Juntti, and T. Matsumoto, "A Tutorial on Lossy Forwarding Cooperative Relaying," *IEEE Communications Surveys Tutorials*, pp. 1–1, 2018.

[15] S. Biswas and A. Chandra, "DF versus AF: Energy consumption comparison for IEEE 802.15.4 networks," in *2014 Sixth International Conference on Communication Systems and Networks (COMSNETS)*, Jan 2014, pp. 1–7.

[16] E. Bjornson, M. Matthaiou, and M. Debbah, "A New Look at Dual-Hop Relaying: Performance Limits with Hardware Impairments," *IEEE Transactions on Communications*, vol. 61, no. 11, pp. 4512–4525, November 2013.

[17] E. Zedini, I. S. Ansari, and M. S. Alouini, "Performance Analysis of Mixed Nakagami- m and Gamma-Gamma Dual-Hop FSO Transmission Systems," *IEEE Photon. J.*, vol. 7, no. 1, pp. 1–20, Feb 2015.

[18] I. S. Ansari, F. Yilmaz, and M.-S. Alouini, "Performance Analysis of Free-Space Optical Links Over Málaga-$\mathcal{M}$ Turbulence Channels with Pointing Errors," *IEEE Trans. Wireless Commun.*, vol. 15, no. 1, pp. 91–102, January 2016.

[19] H. AlQuwaiee, I. S. Ansari, and M. S. Alouini, "On the Performance of Free-Space Optical Communication Systems Over Double Generalized Gamma Channel," *IEEE J. Sel. Areas Commun.*, vol. 33, no. 9, pp. 1829–1840, Sept 2015.

[20] L. Wang, M. Elkashlan, J. Huang, R. Schober, and R. K. Mallik, "Secure Transmission With Antenna Selection in MIMO Nakagami- m Fading Channels," *IEEE Trans. Wireless Commun.*, vol. 13, no. 11, pp. 6054–6067, Nov 2014.

[21] Y. Jiang, J. Zhu, and Y. Zou, "Secrecy outage analysis of multi-user cellular networks in the face of cochannel interference," in *2015 IEEE 14th International Conference on Cognitive Informatics Cognitive Computing (ICCI*CC)*, July 2015, pp. 441–446.

[22] T. Zheng, H. Wang, and J. Yuan, "Physical-Layer Security in Cache-Enabled Cooperative Small Cell Networks Against Randomly Distributed Eavesdroppers," *IEEE Transactions on Wireless Communications*, vol. 17, no. 9, pp. 5945–5958, Sept 2018.

[23] K. An, T. Liang, X. Yan, and G. Zheng, "On the Secrecy Performance of Land Mobile Satellite Communication Systems," *IEEE Access*, vol. 6, pp. 39 606–39 620, 2018.

[24] F. J. Lopez-Martinez, G. Gomez, and J. M. Garrido-Balsells, "Physical-Layer Security in Free-Space Optical Communications," *IEEE Photon. J.*, vol. 7, no. 2, pp. 1–14, April 2015.

[25] X. Sun and I. B. Djordjevic, "Physical-Layer Security in Orbital Angular Momentum Multiplexing Free-Space Optical Communications," *IEEE Photon. J.*, vol. 8, no. 1, pp. 1–10, Feb 2016.

[26] M. J. Saber and S. M. S. Sadough, "On Secure Free-Space Optical Communications Over Málaga Turbulence Channels," *IEEE Wireless Communications Letters*, vol. 6, no. 2, pp. 274–277, April 2017.

[27] H. Lei, Z. Dai, I. S. Ansari, K. H. Park, G. Pan, and M. S. Alouini, "On Secrecy Performance of Mixed RF-FSO Systems," *IEEE Photon. J.*, vol. 9, no. 4, pp. 1–14, Aug 2017.

[28] A. H. A. El-Malek, A. M. Salhab, S. A. Zummo, and M. S. Alouini, "Enhancing Physical Layer Security of Multiuser SIMO Mixed RF/FSO Relay Networks with Multi-Eavesdroppers," in *2016 IEEE Globecom Workshops (GC Wkshps)*, Dec 2016, pp. 1–7.

[29] E. Illi, F. E. Bouanani, D. B. D. Costa, F. Ayoub, and U. S. Dias, "Dual-hop mixed rf-uow communication system: A phy security analysis," *IEEE Access*, vol. 6, pp. 55 345–55 360, 2018.

[30] P. Wang and X. Zhang, "Energy-efficient relay selection for QoS provisioning in MIMO-based underwater acoustic cooperative wireless sensor networks," in *2013 47th Annual Conference on Information Sciences and Systems (CISS)*, March 2013, pp. 1–6.

[31] A. Khan, I. Ali, A. U. Rahman, M. Imran, Fazal-E-Amin, and H. Mahmood, "Co-EEORS: Cooperative Energy Efficient Optimal Relay Selection Protocol for Underwater Wireless Sensor Networks," *IEEE Access*, vol. 6, pp. 28 777–28 789, 2018.

[32] P. Pai and M. Z. A. Khan, "Comparison of SC and MRC receiver complexity for three antenna diversity systems," in *2008 24th Biennial Symposium on Communications*, June 2008, pp. 302–305.

[33] E. Illi, F. E. Bouanani, D. B. da Costa, F. Ayoub, and U. S. Dias, "On the Secrecy Performance of Mixed RF/UOW Communication System," in *GLOBECOM'18 - IEEE Global Communications Conference*, Dec 2018.

[34] M.-K. Simon and M.-S. Alouini, *Digital Communication Over Fading Channels*. New York: John Wiley and Sons, 2005.

[35] I. S. Gradshteyn and I. M. Ryzhik, *Table of Integrals, Series, and Products: Seventh Edition*. Burlington, MA: Elsevier, 2007.

[36] C. M. Lu and W. H. Lans, "Approximate BER performance of generalized selection combining in Nakagami-m fading," *IEEE Communications Letters*, vol. 5, no. 6, pp. 254–256, June 2001.

[37] F. Yilmaz and M. S. Alouini, "Product of shifted exponential variates and outage capacity of multicarrier systems," in *2009 European Wireless Conference*, May 2009, pp. 282–286.

[38] I. W. Research, *Mathematica Edition: version 11.3*. Champaign, Illinois: Wolfram Research, Inc., 2018.

[39] E. Illi, F. E. Bouanani, and F. Ayoub, "A performance study of a hybrid 5G RF/FSO transmission system," in *2017 International Conference on Wireless Networks and Mobile Communications (WINCOM)*, Nov 2017, pp. 1–7.

[40] A. A. Kilbas and M. Saigo, *H-Transforms: Theory and Applications*. Boca Raton, Florida, US: CRC Press, 2004.

[41] Z. G. W. Popoola and S. Rajbhandari, *Optical Wireless Communications: System and Channel Modelling with MATLAB*. Boca Raton: CRC Press, 2013.